4. Application case study

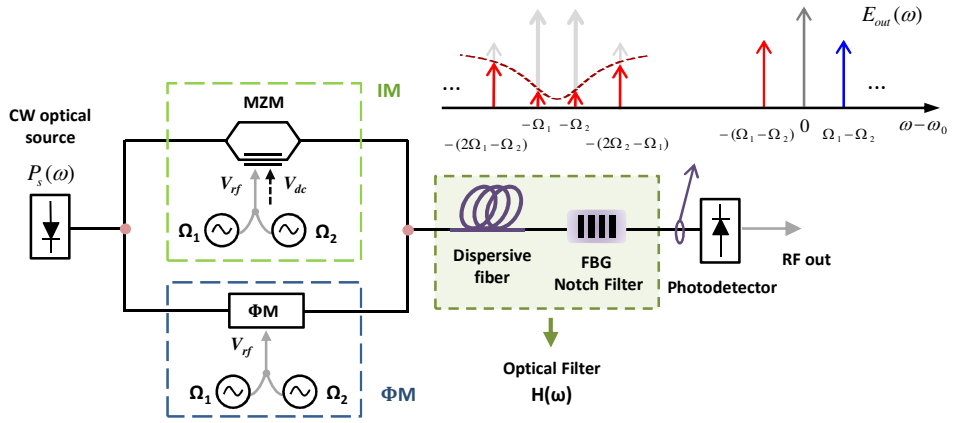

Fig. 5. Schematic of a filtered MWP link composed of a dispersive fiber link and a FBG-based notch filter.

As a proof of concept, the reported analytical model will be applied to the performance evaluation of an interesting application case, represented in Fig. 5, composed of a dispersive fiber link followed by a notch filter implemented by a FBG, the spectrum of which is provided by experimental measurement. The functionality of the selective optical filter is to suppress the lower-frequency sideband of the microwave signal as it has been depicted in the upper region of Fig. 5. We will consider both standard silica SMF and 62.5/125-μm parabolic-core graded-index MMF links characterized by an intrinsic loss α^0 = 0.2 dB/km and $\beta^{''}$ = −21 psec^2/km for an optical wavelength of 1.55 μm. The modal attenuation α_m^0, the modal delay time τ_m the light injection coefficient C_{mm} and the modal coupling coefficient G_{mm} have been calculated following the formulas previously presented in Ref [17]. The equivalent optical transfer function $H(\omega)$ will result in a cascade of the FBG frequency response and the transfer function given by Eq. (51) and Eq. (54) respectively for the SMF and MMF links.

Both intensity and phase modulation with direct-detection will be considered for a modulating signal comprising two RF tones for which we have selected two different combinations of the microwave frequencies f_1 and f_2, involving two different suppression levels for the red-shifted frequency sideband of the electrical signal: an attenuation of around 38.5 dB for both tones if their frequencies are placed at the center of the notch response (namely case FBG$_A$), f_1^A = 12 and f_2^A = 10 GHz; while values around 8 and 11 dB when they are placed in the area corresponding to the frequency slopes of the filter response (referred as case FBG$_B$), f_1^B = 16 and f_2^B = 7 GHz. The measured magnitude and phase shift frequency responses of the FBG operating in transmission are shown in Fig. 6 in function of the difference between the microwave frequency f and the filter central frequency f_c. The relative location of the RF tones in the FBG response has been included in Fig. 6 for both filtering conditions FBG$_A$ and FBG$_B$.

#151909 - $15.00 USD Received 27 Jul 2011; revised 28 Aug 2011; accepted 31 Aug 2011; published 23 Sep 2011
(C) 2011 OSA

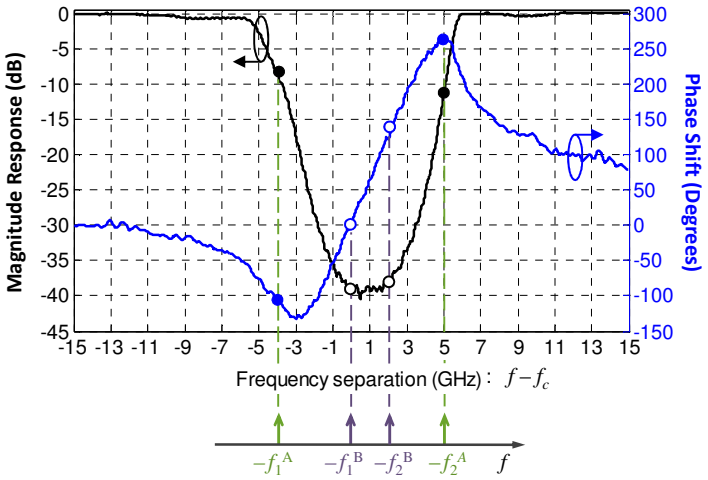

Fig. 6. Measured FBG transmission magnitude and phase shift frequency responses.

The performance analysis of the proposed filtered MWP link is accomplished firstly by evaluating the RF Link Gain frequency response for the particular case where only the dispersive optical fiber is present. With the objective of showing the coincidence of the computed results with previously reported expressions for this well-known radio over fiber system, we report a comparison between singlemode propagation, represented in Fig. 7 (a) and (b), and multimode transmission, gathered in Fig. 7 (c) - (f), for different application contexts. The dependence of the link gain on the coherence properties of a Gaussian optical source is corroborated by comparing two representative RMS spectral linewidths, Δf = 10 MHz and 4 GHz, where $\Delta W = 2\pi \cdot \Delta f$. The influence of both the CSE and the multimode transversal filtering effect is evaluated by considering different link lengths, L = 5 km, [Fig. 7 (a), (c), (e)], and L = 20 km, [Fig. 7 (b), (d), (f)]. The following parameters are kept fixed: V_π = 6.9 V, quadrature MZM bias point $\phi_{dc} = \pi/2$, I_{dc} = 5 mA and $R_{in} = R_{out}$ = 50 Ω.

We initiate the G_{RF} evaluation for this well-known dispersive fiber link by analyzing the main differences in between the frequency responses offered by the two modulation formats under consideration. As it was expected, we can see at first glance for every example gathered in Fig. 7, the influence of the CSE and how the gain notches are produced at different frequency locations when comparing both modulation techniques. This characteristic can be derived for SMF from Eq. (52) and (53) and also for MMF according to Eq. (55) and (56). These equations predict also the 12-dB difference between the peak levels, mainly appreciable for L = 20 km, in total agreement with [5]. It should be also mentioned that, as predicted, in principle transmission regions can be identified in both single and multimode propagation for L = 5 km while for L = 20 km the effect of the carrier suppression term cannot be overlooked.

The reported expression for G_{RF} in terms of the spectral density function of the optical source can be employed to efficiently investigate the effect of its coherence properties on our system performance. As we can observe, the source dependent low-pass frequency term present in Eq. (52) and (53) for the SMF and in Eq. (55) and (56) for the MMF becomes patent when we increase the source spectral linewidth from Δf = 10 MHz, typical of a distributed feedback laser (DFB), up to a value of Δf = 9 GHz, for a 20 km link length. The same low-pass behavior, previously discussed in [17], occurs for both single and multimode fibers.

#151909 - $15.00 USD Received 27 Jul 2011; revised 28 Aug 2011; accepted 31 Aug 2011; published 23 Sep 2011
(C) 2011 OSA

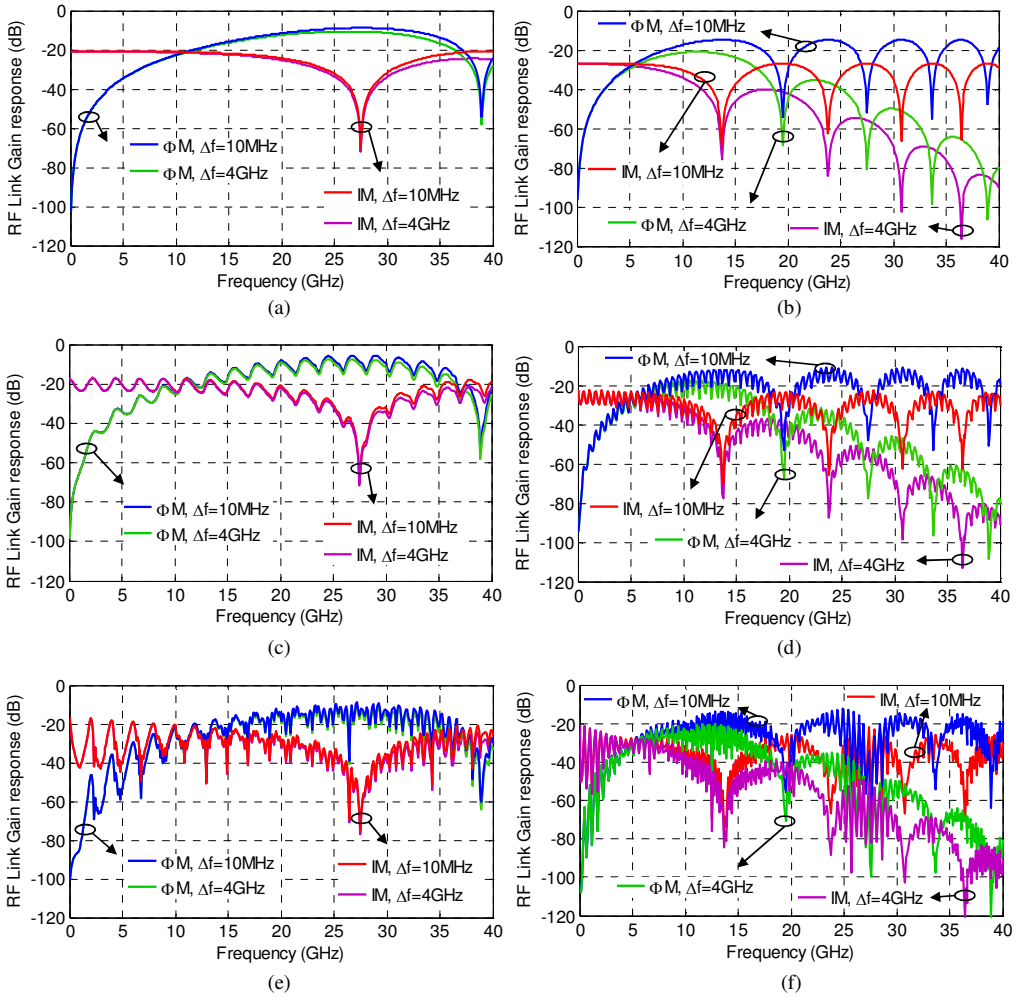

Fig. 7. G_{RF} response in a dispersive link for intensity (IM) and phase (ΦM) modulation with direct detection. (a) 5 km SMF. (b) 20 km SMF. (c) 5 km MMF and (d) 20 km MMF with central launching. (e) 5 km MMF and (f) 20 km MMF with uniform launching.

Finally, we will analyze the transversal filtering effect [17] that intrinsically characterizes the multimode propagation for different intensity launch conditions. Figure 7 (c) and (d) correspond to a selective central assignment of the light injection coefficient C_{mm} where the low-order mode groups have been excited following a Gaussian distribution, while Fig. 7 (e) and (f) refer to a uniform overfilled launch (OFL) condition. The comparison between both injection techniques corroborates that central launching results into a reduction in the depth of the transversal filtering notches as a consequence of forcing less intermodal dispersion. In this case, most of the energy is concentrated in the axial core region what subsequently reduces the effect of modal dispersion from the coupling of the high-order modes to the lower ones.

If a notch filter is introduced in order to suppress the red-shifted frequency sideband of the modulating signal prior to photodetection, CSE is expected to be completely avoided, as it actually occurs for Single Sideband Modulation links. Indeed, the application of our model to the case when the lower-frequency modulating band is attenuated by more than 38 dB, (FBG_A), results in a complete reduction of the typical CSE notches for both modulation choices. This behavior is displayed in Fig. 8 (a) for the SMF link and in Fig. 8 (b) for the MMF link with central launching, showing a comparison between the cases of maximum,

#151909 - $15.00 USD Received 27 Jul 2011; revised 28 Aug 2011; accepted 31 Aug 2011; published 23 Sep 2011
(C) 2011 OSA

FBG_A, and minimum, FBG_B, attenuation. We can also observe how a reduction in the level of red-shifted frequency sideband suppression implies a minor CSE compensation (FBG_B). Note that the deep notch experienced in the baseband region for IM and in the vicinity of 5 GHz for ΦM is not actually related to the CSE, but to the fact that the optical carrier falls also into the notch of the FBG response when the electrical frequency is located into those regions.

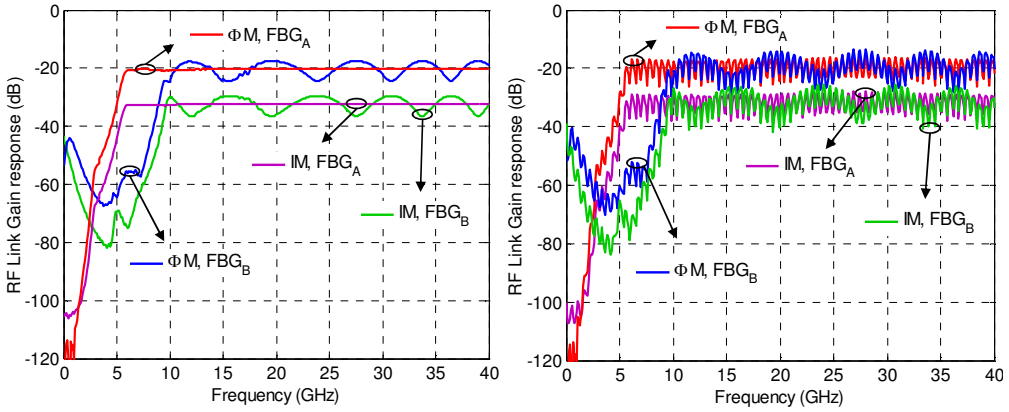

Fig. 8. G_{RF} response in a link comprising a dispersive fiber and a FBG notch filter comparing different sideband suppression levels (FBG_A and FBG_B), for intensity (IM) and phase (ΦM) modulation with direct detection. (a) 20 km SMF. (b) 20 km MMF with central launching.

The usefulness of our model becomes even clearer when the performance evaluation of filtered MWP links requires the analysis of the nonlinear distortion. In this context, Fig. 9 illustrates the analysis of the RF photodetected power for the modulating signal at Ω_1, (from $P_{RF}|_{out}(\Omega_1)$ in Eq. (7) and (26)), the IMD_2 term at Ω_1–Ω_2, (from $P_{RF}|_{out}(\Omega_1$–$\Omega_2)$ in Eq. (15) and (34)), and the IMD_3 term at $2\Omega_1$–Ω_2, (from $P_{RF}|_{out}(2\Omega_1$–$\Omega_2)$ in Eq. (18) and (37)), versus the RF modulator input power when the filtered MWP link consists of a 20 km SMF link and a FBG applying maximum suppression level (case FBG_A). The results computed for intensity modulation are plotted in solid lines while the ones obtained for phase modulation are plotted in dashed lines. Here a low-linewidth laser characterized by Δf = 10 MHz has been assumed. Apart from the predicted output level increase when ΦM is applied, we can appreciate that the computed OIP_2 and OIP_3 are respectively around 7 and 4 dB higher than for IM, again in complete agreement with [5]. For the computation of the total output noise spectral density N_{tot} , apart from the output contribution due to thermal noise at the input and thermal noise at the output for T = 290 K and the contribution of shot noise, we have assumed RIN_{laser} = −160 dBm/Hz, obtaining similar dynamic range figures for both modulation schemes: $SFDR_2$ = 81,75 dB·$Hz^{1/2}$ and $SFDR_3$ = 110,57 dB·$Hz^{2/3}$ for intensity modulation, while $SFDR_2$ = 83,12 dB·$Hz^{1/2}$ and $SFDR_3$ = 110,26 dB·$Hz^{2/3}$ for phase modulation.

#151909 - $15.00 USD Received 27 Jul 2011; revised 28 Aug 2011; accepted 31 Aug 2011; published 23 Sep 2011
(C) 2011 OSA

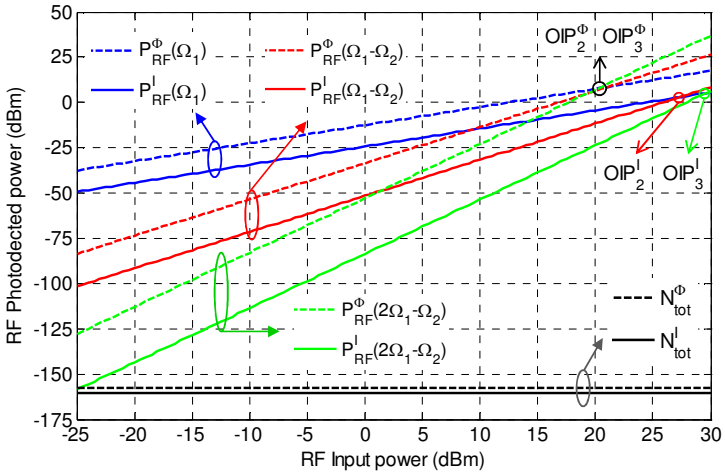

Fig. 9. RF photodetected power for the signal, IMD_2 and IMD_3 terms and output noise level as function of the input RF power for a link comprising a dispersive 20 km SMF and a FBG notch filter (maximum attenuation: FBG_A) when employing a low-linewidth laser, $\Delta f = 10$ MHz.

5. Conclusions

We have developed a general analytical propagation model for externally modulated *filtered MWP links*, a novel concept in which the effect of all intermediate optical components can be lumped into an optical transfer function $H(\omega)$ connecting the input to the output of the microwave system. The principal advantage of our model relies on the global character of the described filtered MWP link as it works under very general conditions for the coherence properties of the optical source and allows the analysis of both intensity and/or phase modulation techniques. This approach provides also the expressions leading to the computation of the main figures of merit, RF link gain, noise figure and spurious free dynamic range, enabling in consequence the performance evaluation of a wide range of complex MWP systems.

As a proof of principle, we have particularized the derived closed-form expressions to different well-known examples widely employed by the MWP community leading to a coincidence between the figures of merit formulas provided by this paper with those previously reported in the literature. With the purpose of illustrating the applicability of our model we have also computed the performance metrics of a non-standard radio over fiber system. The extension of the term *filtered MWP links* is envisaged to cover also a variety of fields including non-linear characterization of both amplitude and group delay ripples in chirped FBGs applied to microwave photonic filters, the design of complimentary optical filters in frequency discrimination systems for dynamic range optimization as well as multiport WDM optical distribution networks.

Acknowledgments

The authors wish to acknowledge the financial support given by the Research Excellency Award Program GVA PROMETEO 2008/092.

#151909 - $15.00 USD Received 27 Jul 2011; revised 28 Aug 2011; accepted 31 Aug 2011; published 23 Sep 2011
(C) 2011 OSA